Cellular/Molecular

Ca^{2+}-Dependent Facilitation of $Ca_v1.3$ Ca^{2+} Channels by Densin and Ca^{2+}/Calmodulin-Dependent Protein Kinase II

Meagan A. Jenkins,[1]* Carl J. Christel,[2]* Yuxia Jiao,[4] Sunday Abiria,[4] Kristin Y. Kim,[2] Yuriy M. Usachev,[3] Gerald J. Obermair,[5] Roger J. Colbran,[4] and Amy Lee[2]

[1]Department of Pharmacology, Emory University, Atlanta, Georgia 30322, Departments of [2]Molecular Physiology and Biophysics and [3]Pharmacology, University of Iowa, Iowa City, Iowa 52242, [4]Department of Molecular Physiology and Biophysics, Vanderbilt University, Nashville, Tennessee 37232, and [5]Department of Physiology and Medical Physics, Innsbruck Medical University, A-6020 Innsbruck, Austria

Ca_v1 (L-type) channels and calmodulin-dependent protein kinase II (CaMKII) are key regulators of Ca^{2+} signaling in neurons. CaMKII directly potentiates the activity of $Ca_v1.2$ and $Ca_v1.3$ channels, but the underlying molecular mechanisms are incompletely understood. Here, we report that the CaMKII-associated protein densin is required for Ca^{2+}-dependent facilitation of $Ca_v1.3$ channels. While neither CaMKII nor densin independently affects $Ca_v1.3$ properties in transfected HEK293T cells, the two together augment $Ca_v1.3$ Ca^{2+} currents during repetitive, but not sustained, depolarizing stimuli. Facilitation requires Ca^{2+}, CaMKII activation, and its association with densin, as well as densin binding to the $Ca_v1.3$ α_1 subunit C-terminal domain. $Ca_v1.3$ channels and densin are targeted to dendritic spines in neurons and form a complex with CaMKII in the brain. Our results demonstrate a novel mechanism for Ca^{2+}-dependent facilitation that may intensify postsynaptic Ca^{2+} signals during high-frequency stimulation.

Introduction

CaMKII is a serine-threonine protein kinase that is activated by postsynaptic elevations in Ca^{2+} and plays a central role in synaptic plasticity (Hudmon and Schulman, 2002; Lisman et al., 2002; Colbran and Brown, 2004; Griffith, 2004). Ca_v1 channels mediate L-type Ca^{2+} currents that can regulate CaMKII activation in dendritic spines (Lee et al., 2009), propagation in dendrites (Rose et al., 2009), and coupling to gene transcription (Wheeler et al., 2008) and synaptic plasticity (Yasuda et al., 2003; Lee et al., 2009). Functional interactions of Ca_v1 and CaMKII may involve tethering of CaMKII to the Ca_v1 channel complex. CaMKII binds to and phosphorylates the main $Ca_v1.2$ α_1 (Hudmon et al., 2005) and auxiliary β subunits (Grueter et al., 2006, 2008). These interactions augment cardiac $Ca_v1.2$ currents in a feedback process known as Ca^{2+}-dependent facilitation (CDF) (Dzhura et al., 2000; Wu et al., 2001; Hudmon et al., 2005; Grueter et al., 2006). CaMKII also causes voltage-dependent facilitation (VDF) of $Ca_v1.2$ currents in response to strong depolarizations (Lee et al., 2006).

Due to their distinct biophysical properties (Koschak et al., 2001; Scholze et al., 2001; Xu and Lipscombe, 2001; Helton et al., 2005), $Ca_v1.3$ and $Ca_v1.2$ may play different roles in neurons (Calin-Jageman and Lee, 2008). $Ca_v1.3$ channels regulate spontaneous firing of substantia nigra dopaminergic neurons (Chan et al., 2007; Puopolo et al., 2007), upstate potentials in striatal medium spiny neurons (Olson et al., 2005), and processes underlying fear conditioning (McKinney and Murphy, 2006) and depression-like behavior (Sinnegger-Brauns et al., 2004). Therefore, $Ca_v1.3$ modulation by CaMKII and other factors may have evolved to meet the unique signaling demands of this channel in neurons. Although insulin-like growth factor 1 can potentiate $Ca_v1.3$ currents by a mechanism that requires Ca^{2+} release from intracellular stores and CaMKII activity (Gao et al., 2006b), the role of CaMKII in direct feedback regulation of $Ca_v1.3$ channels is unknown.

Here, we describe an unexpected mechanism for $Ca_v1.3$ modulation by CaMKII involving the PDZ [postsynaptic density-95 (PSD-95)/Discs large/zona occludens-1 (ZO-1)] domain-containing protein densin. Densin is a member of the leucine-rich repeat and PDZ-domain-containing proteins (Bilder et al., 2000) and is localized in the postsynaptic density (Apperson et al., 1996) and binds to and is phosphorylated by CaMKII (Strack et al., 2000; Walikonis et al., 2001). Densin may scaffold other postsynaptic proteins, including Shank (Quitsch et al., 2005), δ-catenin (Izawa et al., 2002), and MAGUIN (Ohtakara et al., 2002), and promotes branching of dendrites in cultured neurons (Quitsch et al., 2005). We showed previously that the related protein erbin enhances voltage-dependent facilitation of $Ca_v1.3$ (Calin-Jageman et al., 2007). Like erbin, densin binds to the C terminus (CT) of the $Ca_v1.3$ α_1 subunit but alone does not affect $Ca_v1.3$ properties. When coexpressed with CaMKII, densin facilitates $Ca_v1.3$ Ca^{2+} currents during high-frequency stimulation. Densin and $Ca_v1.3$ are targeted to dendritic spines and together associate with CaMKII in the hippocampus. Our results show that densin

Received Sept. 2, 2009; revised Feb. 12, 2010; accepted Feb. 19, 2010.

This work was supported by grants from the National Institutes of Health (HL087120, DC009433 to A.L.; MH63232 to R.J.C.; NS054614 to Y.M.U.; and T32 HL07121 to C.J.C.), the American Heart Association (A.L.), the Israel Binational Science Foundation (A.L.), and the Austrian Science Fund (P17807-B05 to G.J.O.). We thank Diane Lipscombe and Randy Hall for cDNAs, Jörg Striessnig for $Ca_v1.3$ knock-out mice, and Irina Calin-Jageman for help in generating the HA-tagged $Ca_v1.3$.

*M.A.J. and C.J.C. contributed equally to this work.

Correspondence should be addressed to Amy Lee, Department of Molecular Physiology and Biophysics, University of Iowa, 5-611 Bowen Science Building, 51 Newton Road, Iowa City, IA 52242. E-mail: amy-lee@uiowa.edu.

DOI:10.1523/JNEUROSCI.4367-09.2010

 0270-6474/10/305125-11$15.00/0

functionally recruits CaMKII to $Ca_v1.3$ channels, which causes frequency-dependent facilitation of $Ca_v1.3$ Ca^{2+} signals that may regulate neuronal excitability.

Materials and Methods

cDNAs. $Ca_v1.3$ channels consisted of rat $\alpha_1$1.3 (containing exon 42, GenBank #AF3700010, in pCDNA6 from D. Lipscombe, Brown University, Providence, RI), β_{1b} (GenBank #NM017346), and $\alpha_2\delta$ (GenBank #M21948). The following cDNAs were described previously: FLAG- and GST-tagged $\alpha_1$1.3 constructs (Calin-Jageman et al., 2007); CaMKIIα, CaMKIIαT286A (Brickey et al., 1990; McNeill and Colbran, 1995); GFP-densin and GFP-densin Δ483-1377 (Jiao et al., 2008); His-densin PDZ (Fam et al., 2005); and pβA-eGFP (Obermair et al., 2004). For GFP-densin ΔPDZ, the PDZ domain-encoding region (aa 1452-1542) was deleted by PCR amplification and ligation into *Bgl*II and *Sac*II sites of pEGFP (Clontech, BD BioSciences).

For external hemagglutinin (HA) epitope-tagged $\alpha_1$1.3, the sequence for the HA tag was cloned into the extracellular loop connecting IIS5-IIS6 according to a similar strategy for $\alpha_1$1.2 described previously (Altier et al., 2002). The insertion of the HA tag had no effects on channel properties as assessed by electrophysiological recordings of transfected HEK293T cells (data not shown). To facilitate neuronal expression HA-$\alpha_1$1.3 was subcloned into the pβA-PL expression vector (Obermair et al., 2010) in a two-step procedure. First, a *Hin*dIII–*Sal*I fragment (3303 bp) containing the 5′ coding sequence of $\alpha_1$1.3 was cloned into the corresponding restriction sites of pβA-PL. Second, the *BsiWI*–*Sac*II fragment (6019 bp) of HA-$\alpha_1$1.3 was ligated together with a 25 bp *Sac*II–*Spe*I linker into the *BsiWI* and *Xba*I sites of the intermediate construct, eliminating *Spe*I and *Xba*I recognition sequences and yielding pβA-HA-$\alpha_1$1.3. The construct was verified by sequencing before use (MWG-Biotech).

Antibodies. Goat $\alpha_1$1.3 antibodies (Calin-Jageman et al., 2007) and goat densin antibodies (Ab650) (Jiao et al., 2008) were characterized previously. Rabbit $\alpha_1$1.3 antibodies (Ab144) were raised against a synthetic peptide corresponding to $\alpha_1$1.3 N-terminal sequence (MQHQRQQQEDHANEANYARGTRKC; Covance Research Products). Characterization of Ab144 specificity is described in supplemental Figure 1, available at www.jneurosci.org as supplemental material. Briefly, by immunofluorescence and Western blot, these antibodies labeled HEK293T cells transfected with $Ca_v1.3$ but not untransfected cells (Fig. S1*A*,*B*, available at www.jneurosci.org as supplemental material). In addition, Ab144 recognized a protein consistent in size with $\alpha_1$1.3 in hippocampal lysates of wild-type but not $Ca_v1.3$ knock-out mice (provided by Jörg Striessnig, University of Innsbruck, Innsbruck, Austria) (Fig. S1*C*, available at www.jneurosci.org as supplemental material). Other antibodies used were as follows: mouse monoclonal antibodies against CaMKIIα (Affinity Bioreagents), FLAG (Sigma-Aldrich), and GFP (Santa Cruz Biotechnology); and rabbit polyclonal antibodies against densin (Santa Cruz Biotechnology) and hexahistidine (anti-His) antibodies (Santa Cruz Biotechnology).

For immunofluorescence of cultured neurons, the following antibodies were used: rat anti-HA (monoclonal, clone 3F10, Roche Diagnostics, 1:100), mouse anti-PSD-95 (monoclonal, clone 6G6–1C9, Affinity Bioreagents, 1:1000), rabbit polyclonal anti-GFP (1:20,000; Invitrogen), goat anti-rabbit Alexa 488 (1:2000), goat anti-mouse Alexa 594 (1:4000), and goat anti-rat Alexa 594 (Invitrogen, 1:4000).

Cell culture and transfection. Human embryonic kidney cells (HEK293) or HEK293 cells transformed with SV40 T-antigen (HEK293T) were maintained in DMEM with 10% fetal bovine serum (Invitrogen) at 37°C in a humidified atmosphere with 5% CO_2. Cells were grown to ~80% confluence and transfected using Gene Porter reagent (Gene Therapy Systems) or Fugene (Roche). For pull-down assays, cells were transfected with GFP-densin (6 μg). For coimmunoprecipitation of GFP-densin and $Ca_v1.3$, cells were transfected with cDNAs encoding $Ca_v1.3$ [FLAG-$\alpha_1$1.3 (6 μg), β_{1b} (2 μg), and $\alpha_2\delta$ (2 μg)] with or without GFP-densin (4 μg). For coimmunoprecipitation of CaMKII and GFP-densin or Δ483-1377, cells were transfected with GFP-densin (7 μg) or GFP-Δ483-1377 (2 μg) and CaMKIIα (1 μg). For electrophysiology, HEK293T cells were transfected with $\alpha_1$1.3 (1.5 μg), β_{1b} (0.5 μg), and $\alpha_2\delta$ (0.5 μg) with or without GFP-tagged densin (0.5 μg) and/or CaMKII (0.5 μg).

Electrophysiological recordings. At least 48 h after transfection, whole-cell patch-clamp recordings of transfected cells were acquired with a HEKA Elektronik (Lambrecht/Pfalz) EPC-8 or EPC-9 patch-clamp amplifier. Data acquisition and leak subtraction using a P/4 protocol were performed with Pulse software (HEKA Elektronik). Extracellular recording solutions contained the following (in mM): 150 Tris, 1 $MgCl_2$, and 10 $CaCl_2$ or 10 $BaCl_2$. Intracellular solutions contained the following (in mM): 140 *N*-methyl-D-glucamine, 10 HEPES, 2 $MgCl_2$, 2 Mg-ATP, and 5 EGTA or 10 BAPTA. The pH of the recording solutions was 7.3, adjusted with methanesulfonic acid. Electrode resistances were 3–4 MΩ in the bath solution. Series resistance was compensated up to 80%. Igor Pro software (Wavemetrics) was used for data analysis. Except for Fig. 7*B* below, data analysis was restricted to $Ca_v1.3$ currents with amplitudes of >250 pA. All averaged data are presented as the mean ± SEM. Statistical significance was determined with either Student's *t* test or ANOVA with *post hoc* analyses, as indicated (SigmaPlot; Systat Software).

Binding assays. GST- and His-tagged fusion proteins were prepared as described previously (Robison et al., 2005; Calin-Jageman et al., 2007). For pull-down assays, GST-$\alpha_1$1.3 CT was immobilized on glutathione agarose beads and incubated with lysate from GFP-densin-transfected HEK293T cells in binding buffer [Tris-buffered saline (TBS; 50 mM Tris-HCl, pH 7.5, 150 mM NaCl), 0.1% Triton X-100, and protease inhibitors (1 mg/ml each of PMSF, pepstatin, aprotinin, and leupeptin)]. Binding reactions proceeded at 4°C for 90 min. Beads were washed three times with binding buffer (1 ml) at 4°C, and bound proteins were eluted, resolved by SDS-PAGE, and transferred to nitrocellulose. Western blotting was performed with appropriate antibodies followed by HRP-conjugated secondary antibodies and enhanced chemiluminescent detection reagents (GE Healthcare). For overlay assays, GST-$\alpha_1$1.3 CT, GST-$\alpha_1$1.3 C-terminal leucine to alanine ($CT_{L\text{-}A}$), or GST (1 μg) was run on a 4–20% SDS-polyacrylamide gel and transferred to nitrocellulose. The membrane was blocked in blocking buffer (2% milk, TBS, 0.1% Tween 20) for 30 min (4°C) before incubation with His-tagged densin-PDZ domain (300 nM in blocking buffer) for 1 h at 4°C. Bound protein was detected by Western blotting with anti-His antibodies.

Coimmunoprecipitation assays. For coimmunoprecipitation from mouse hippocampus, a Triton X-100-soluble fraction (0.5 ml) was prepared as described previously (Abiria and Colbran, 2010) and incubated with 10 μg of either goat IgG or affinity-purified goat antibodies that recognize CaMKII, densin, or $\alpha_1$1.3. After 1 h, 10 μl of protein-G Sepharose (GE Healthcare Bio-Sciences) was added and the incubation continued for ~2 h at 4°C. The resin was rinsed three times in 1 ml of solubilization buffer and bound proteins were analyzed by SDS-PAGE and Western blotting with mouse antibodies to CaMKIIα or rabbit antibodies to densin and $\alpha_1$1.3 (Ab144).

For coimmunoprecipitation of GFP-densin and $\alpha_1$1.3, transfected HEK293T cells were solubilized in lysis buffer (50 mM Tris-HCl, pH 7.5, 150 mM NaCl, 1% NP-40, 0.25% sodium deoxycholate, 1 mM EDTA, and protease inhibitors), incubated at 4°C for 30 min, and subjected to centrifugation at 100,000 × *g* (30 min) to remove insoluble material. The supernatant was incubated with 5 μg $\alpha_1$1.3 antibodies and 50 μl of protein A-Sepharose (50% slurry) for 4 h, rotating at 4°C. After three washes with RIPA buffer (1 ml), proteins were eluted with SDS-containing sample buffer and subjected to SDS-PAGE. Coimmunoprecipitated proteins were detected by Western blotting with specific antibodies as indicated.

For coimmunoprecipitation of CaMKII and densin or Δ483-1377, transfected HEK293 cells were lysed on ice with lysis buffer [2 mM Tris-HCl, pH 7.5, 1% (v/v) Triton X-100, 0.1 mM PMSF, 1 mM benzamidine, 5 mg/L leupeptin, 20 mg/L soybean trypsin inhibitor]. After sonication (2 × 5 s), lysates were incubated at 4°C for 30 min and then centrifuged for 15 min at 10,000 × *g*. NaCl was added into the supernatant with the final concentration as 150 mM and equal aliquots of the supernatants were incubated with 10 μg of densin Ab450 or goat IgG, or goat CaMKIIα antibody overnight at 4°C. After addition of GammaBind

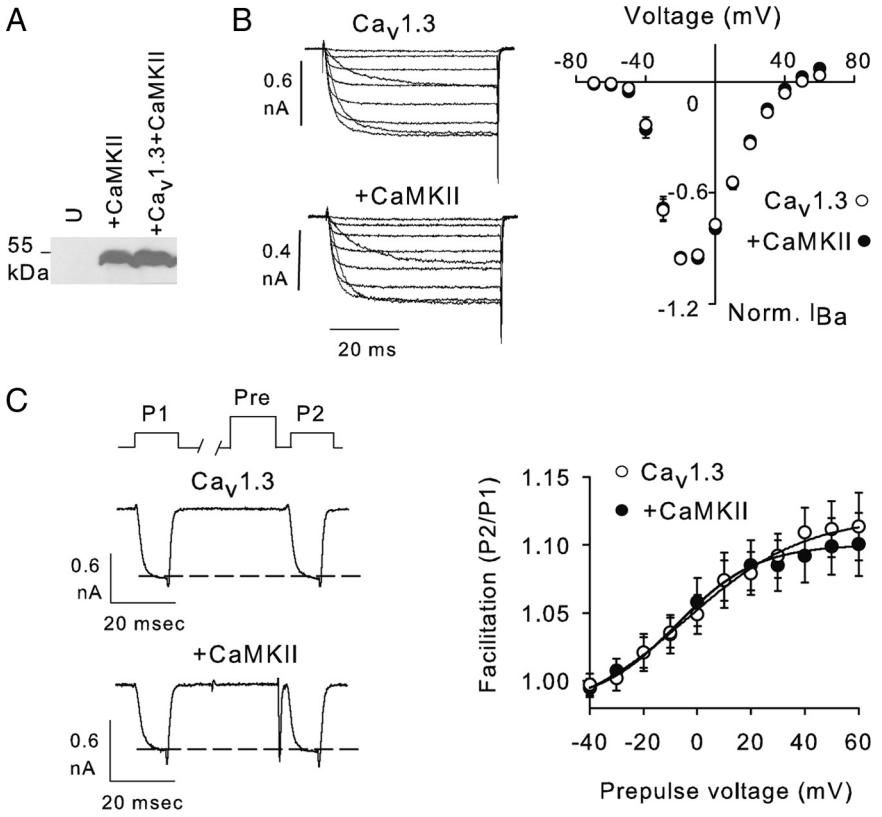

Figure 1. CaMKII does not affect $Ca_v1.3$ activation or voltage-dependent facilitation. ***A***, Western blot with CaMKII antibodies showing CaMKII expression in HEK293T cells transfected with CaMKIIα alone or $+Ca_v1.3$ ($\alpha_1$1.3, β_{1b}, $\alpha_2\delta$) but not untransfected cells (U). ***B***, I_{Ba} were evoked by 50 ms test pulses from -90 to various voltages in HEK293T cells transfected with $Ca_v1.3$ alone ($n = 18$, open circles) or cotransfected with CaMKII ($n = 16$, closed circles). Representative current traces (left) and normalized (Norm.) *I–V* relationship (right) are shown. For $Ca_v1.3$ alone, $V_{1/2} = -26.3 \pm 2.4$ mV, $k = -6.7 \pm 0.5$. For $Ca_v1.3$ plus CaMKII, $V_{1/2} = -26.6 \pm 1.5$ mV, $k = -7.2 \pm 0.3$. ***C***, I_{Ba} was evoked by 10 ms test pulse from -90 to -20 mV before (P1) and after (P2) a 20 ms prepulse (Pre) to various voltages. Left, Voltage protocol and representative test currents using $+60$ mV prepulse. Dashed line indicates initial P1 current amplitude. Right, Facilitation was measured as the ratio of the P2 and P1 test currents and plotted against prepulse voltage for cells transfected with $Ca_v1.3$ alone ($n = 10$) or cotransfected with CaMKII ($n = 12$). By two-way ANOVA, there was no difference in facilitation between groups.

Plus-Sepharose (30 μl of 50% slurry; GE Healthcare), incubations were continued for 2 h at 4°C. Beads were collected by centrifugation and washed at least five times with 1 ml of wash buffer containing 50 mM Tris-HCl, pH 7.5, 1% (v/v) Triton X-100, and 150 mM NaCl. Immune complexes were solubilized in SDS-PAGE sample buffer before electrophoresis and Western blotting. Interpretations of results from coimmunoprecipitation and binding assays were based on at least three independent experiments.

$Ca_v1.3$ and densin targeting in transfected mouse hippocampal neurons. Low-density cultures of hippocampal neurons were prepared from 16.5-d-old embryonic BALB/c mice as described previously (Obermair et al., 2004). The following plasmids (1.5 μg total DNA) were transfected into neurons on day 6 using Lipofectamine 2000 transfection reagent (Invitrogen): GFP-densin (single transfection) and pβA-eGFP and pβA-HA-$\alpha_1$1.3 (cotransfection). Cells were immunostained and analyzed 11–14 d after transfection.

For double-immunolabeling (GFP-densin and PSD-95) neurons were fixed with methanol for 10 min at -20°C and rehydrated in PBS at room temperature. Fixed neurons were incubated in 5% normal goat serum in PBS, 0.2% bovine serum albumin, and 0.2% Triton X-100 (PBS/BSA/Triton) for 30 min. Primary antibodies were applied in PBS/BSA/Triton at 4°C overnight and detected by fluorochrome-conjugated secondary antibodies. For staining of surface-expressed HA-$\alpha_1$1.3, living neurons were incubated with the rat anti-HA antibody for 30 min at 37°C. Then the cultures were rinsed in Hank's buffered saline, fixed in 4% paraformaldeyde/ 4% sucrose for 10 min, blocked with 5% normal goat serum in PBS/BSA/Triton, and incubated with the secondary antibody for 1 h (Obermair et al., 2010). Coverslips were then washed and mounted in *p*-phenylene-diamine-glycerol to retard photobleaching. Preparations were analyzed on an AxioImager microscope (Carl Zeiss) using a 63×, 1.4 numerical aperture (NA) objective. Images were recorded with a cooled CCD camera (SPOT; Diagnostic Instruments) and Metavue image processing software (Universal Imaging). Composite images were arranged in Adobe Photoshop 9 (Adobe Systems) and linear adjustments were performed to correct black level and contrast.

Measurements of intracellular Ca^{2+} concentration ($[Ca^{2+}]_i$). HEK293T cells transfected with $Ca_v1.3$, densin, and CaMKII were loaded with fura-2 (Invitrogen) via the patch pipette (100 μM), which also contained the intracellular recording solution described for electrophysiological recordings. Cells were placed in a flow-through chamber mounted on the stage of an inverted IX-71 microscope (Olympus). Fluorescence was alternately excited at 340 nm (12 nm bandpass) and 380 nm (12 nm bandpass) using the Polychrome IV monochromator (TILL Photonics) via a 40× oil-immersion objective (NA = 1.35, Olympus). Emitted fluorescence was collected at 510 nm (80 nm bandpass) using an IMAGO CCD camera (TILL Photonics). Pairs of 340/380 nm images were sampled at 10 Hz. Fluorescence was corrected for background, as determined in an area that did not contain a cell. Data were processed using TILLvisION 4.0.1.2 (TILL Photonics) and presented as a fluorescence ratio of F_{340}/F_{380}, where F_{340} and F_{380} are fluorescence intensities at the excitation wavelengths 340 and 380 nm, respectively. Averaged data are presented as the mean ± SEM and were statistically compared by *t* test.

Results

CaMKII does not affect $Ca_v1.3$ properties in transfected HEK293T cells

Because of the importance of CaMKII as both regulator and transducer of Ca_v1 Ca^{2+} signals (Dzhura et al., 2000; Wheeler et al., 2008), we tested whether CaMKII directly influences $Ca_v1.3$ function. For this purpose, we compared channel properties in HEK293T cells transfected with $Ca_v1.3$ alone ($\alpha_1$1.3, β_{1b}, and $\alpha_2\delta$) and those cotransfected with $Ca_v1.3$ and CaMKIIα. This isoform of CaMKII was chosen since it is one of the major isoforms of CaMKII in the brain (Colbran and Brown, 2004) and cannot be detected endogenously in HEK293T cells (Fig. 1*A*). We found that CaMKII had no effect on voltage-dependent activation of $Ca_v1.3$ Ba^{2+} currents (I_{Ba}). Parameters describing current–voltage (*I–V*) curves were not different in cells with $Ca_v1.3$ and those with $Ca_v1.3$ plus CaMKII ($p = 0.32$ for k, $p = 0.92$ for $V_{1/2}$, by *t* test) (Fig. 1*B*). Expression of CaMKII also did not affect mean $Ca_v1.3$ current amplitudes (535 ± 78 pA for $Ca_v1.3$ alone, $n = 18$ vs 844 ± 227 pA for plus CaMKII, $n = 16$; $p = 0.18$ by *t* test). While CaMKII enhances VDF of $Ca_v1.2$ (Lee et al., 2006), we did not find the same result for $Ca_v1.3$. VDF was measured as the ratio of the amplitude of I_{Ba} evoked before or after a conditioning prepulse. With this protocol, I_{Ba}

underwent modest VDF that was not further affected by CaMKII ($p = 0.68$) (Fig. 1*C*). We also did not observe any differences in the extent of I_{Ba} inactivation either during sustained or repetitive stimuli (data not shown).

Densin binds to $Ca_v1.3$ α_1 C terminus

In contrast to our findings, previous studies of SH-SY5Y human neuroblastoma cells and cortical neurons implicated CaMKII and release of Ca^{2+} from intracellular stores in the potentiation of $Ca_V1.3$ currents at negative voltages following stimulation with insulin-like growth factor 1 (Gao et al., 2006b). Analogous to the role of cAMP-dependent protein kinase (PKA) anchoring proteins for PKA regulation of Ca_v1 channels (Hulme et al., 2004), feedback modulation of $Ca_v1.3$ by CaMKII may require additional adaptor proteins present in neurons but not HEK293T cells. Densin was considered since it binds to CaMKII (Strack et al., 2000; Walikonis et al., 2001) and contains a type I PDZ domain that could associate with the corresponding recognition site at the distal CT of $\alpha_1$1.3 (Fig. 2*A*). Consistent with this possibility, GFP-tagged densin coimmunoprecipitated with FLAG-tagged $\alpha_1$1.3 in HEK293T cells (Fig. 2*B*) and bound *in vitro* to GST-tagged proteins containing the $\alpha_1$1.3 CT, but not GST (Fig. 2*C*). To test the importance of the PDZ-binding sequence of $\alpha_1$1.3 for the interaction, we mutated the $CT_{L\text{-}A}$, which should prevent PDZ binding (Songyang et al., 1997; Calin-Jageman et al., 2007). Unlike for the wild-type $\alpha_1$1.3 CT, the densin PDZ domain did not bind to $CT_{L\text{-}A}$ (Fig. 2*D*). These results confirmed a direct interaction of densin with the $\alpha_1$1.3 CT PDZ-binding sequence.

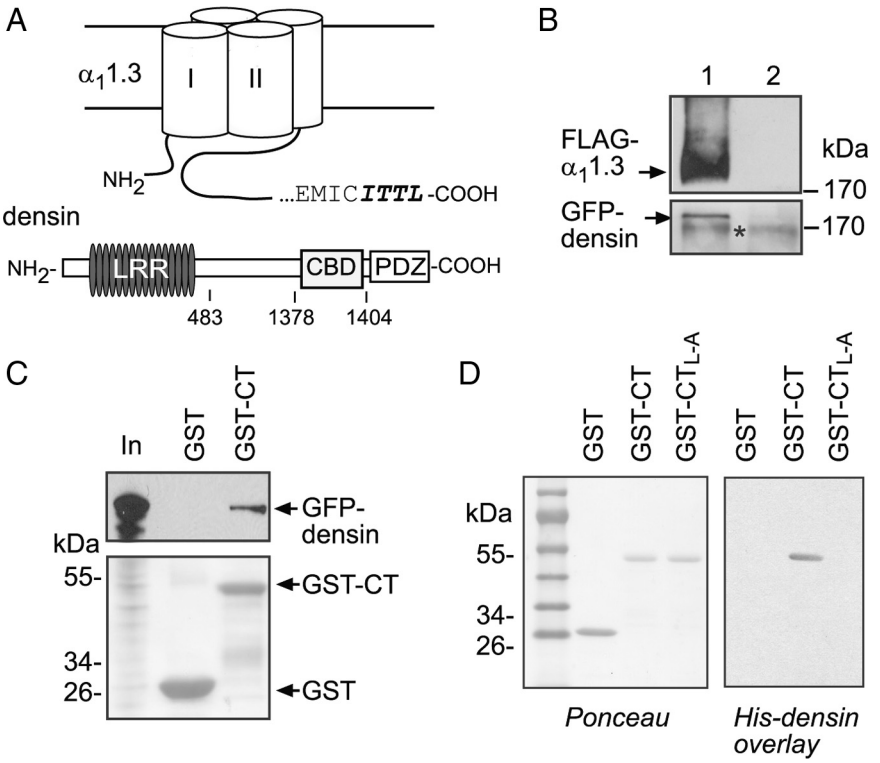

Figure 2. Densin binds to $\alpha_1$1.3. ***A***, Top, Rat $\alpha_1$1.3 with C-terminal type I PDZ-domain indicated with italics; bottom, rat densin with leucine-rich region (LRR), CaMKII-binding domain (CBD), and PDZ domain (not drawn to scale). Numbers indicate amino acid boundaries. ***B***, Coimmunoprecipitation of GFP-densin with FLAG-tagged $\alpha_1$1.3. Lysates from HEK293T cells cotransfected with $Ca_v1.3$ (FLAG-$\alpha_1$1.3, β_{1b}, $\alpha_2\delta$) and GFP-densin (lane 1) or transfected with GFP-densin alone (lane 2) were incubated with goat $\alpha_1$1.3 antibodies. Immunoprecipitated proteins were detected by Western blotting with FLAG (top) or GFP (bottom) antibodies. Asterisk indicates nonspecific band detected by GFP antibody. ***C***, Pull-down of GFP-tagged densin by GST-tagged $\alpha_1$1.3 CT (GST-CT). GST (lane 2) or GST-CT (lane 3) was immobilized on glutathione-agarose beads and incubated with lysates from HEK293T cells transfected with GFP-densin. Top, Western blot with GFP antibody. Bottom, GST-CT and GST protein used for pull-down are indicated in the Ponceau-stained blot. Lane 1 (In) shows ~5% of the GFP-transfected cell lysate used in the assay. ***D***, Binding of His-tagged densin PDZ-domain to GST-CT but not to GST or CT with mutation in PDZ-binding sequence ($GST\text{-}CT_{L\text{-}A}$) in protein overlay assay. GST proteins were separated by SDS-PAGE and transferred to nitrocellulose, which was incubated with His-densin. Left, Ponceau staining shows levels of GST proteins used in the assay. Right, Western blot with anti-His antibodies shows binding of His-densin PDZ only to GST-CT.

We next investigated the potential for densin and $Ca_v1.3$ to interact in neurons. We first tested whether $Ca_v1.3$ channels and densin were associated with the same subcellular compartments in neurons. To restrict analysis to plasma membrane channels, we analyzed the localization of transfected HA-tagged $\alpha_1$1.3 in which the HA tag was inserted in an extracellular domain of $\alpha_1$1.3. Immunofluorescence with HA antibodies applied to live neurons cotransfected with eGFP and HA-$\alpha_1$1.3 revealed a punctate distribution for $Ca_v1.3$ along the shaft and spines throughout the dendritic arbor (Fig. 3*A*). GFP-tagged densin showed a similar distribution, which was predominantly postsynaptic as indicated by colocalization with PSD-95 (Fig. 3*B*).

Unfortunately, we could not determine whether both GFP-densin and $Ca_v1.3$ were colocalized since cotransfection of the corresponding cDNAs was deleterious to neuronal survival (data not shown). Therefore, we tested for a physical interaction between densin and $Ca_v1.3$ by coimmunoprecipitation. The $\alpha_1$1.3 antibodies, but not control IgG, coimmunoprecipitated densin with $\alpha_1$1.3 from solubilized mouse hippocampal membrane extracts (Fig. 3*C*). In the reverse approach, $\alpha_1$1.3 was similarly brought down by densin antibodies (Fig. 3*D*). Consistent with a role for densin in scaffolding CaMKII to the channel complex, CaMKII was coimmunoprecipitated regardless of whether antibodies against densin or $\alpha_1$1.3 were used (Fig. 3*C*,*D*). Moreover, CaMKII antibodies specifically coimmunoprecipitated both densin and $\alpha_1$1.3 (Fig. 3*E*), despite a weak nonspecific interaction of CaMKII with the control IgG, which was most likely due to abundance of CaMKII in hippocampal extracts. Collectively, these results support the existence of a ternary complex comprised of densin, CaMKII, and $Ca_v1.3$ channels in the hippocampus.

Densin and CaMKII cause Ca^{2+}-dependent facilitation of $Ca_v1.3$ Ca^{2+} currents

To test whether densin may functionally recruit CaMKII for modulation of $Ca_v1.3$, we analyzed the effect of cotransfecting densin plus CaMKII with $Ca_v1.3$ in HEK293T cells. While densin plus CaMKII did not affect voltage-dependent activation or facilitation of $Ca_v1.3$ (data not shown), they significantly increased the amplitude of $Ca_v1.3$ Ca^{2+} currents (I_{Ca}) during trains of depolarizations (100 Hz) (Fig. 4*A*). With this voltage protocol, I_{Ca} in cells transfected with $Ca_v1.3$ alone inactivates rapidly (~40% within 50 ms) (Fig. 4*A*), due to Ca^{2+}-dependent inactivation (CDI) mediated by calmodulin (Yang et al., 2006). In cells cotransfected with densin plus CaMKII, I_{Ca} inactivated signifi-

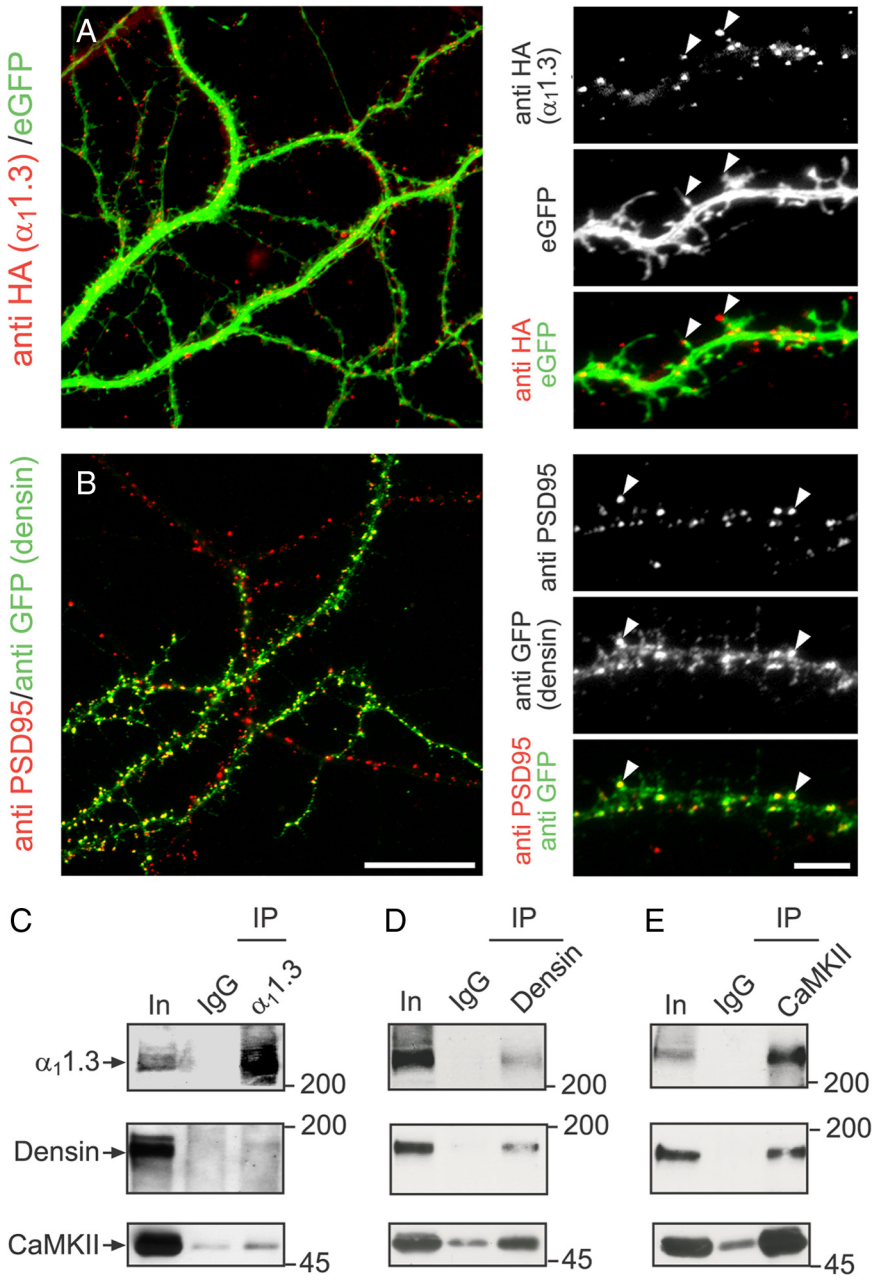

Figure 3. Densin and $Ca_v1.3$ are targeted to dendritic spines in neurons and form a ternary complex with CaMKII in the hippocampus. ***A***, ***B***, Epifluorescence images of immunofluorescently labeled transfected mouse hippocampal neurons in low-density culture. Grayscale images show fluorescence due to individual fluorophores; merged images are shown in color with regions of colocalization appearing yellow. ***A***, Dendritic tree of neuron [17 days *in vitro* (DIV)] cotransfected with HA-$\alpha_1$1.3 and eGFP after live-cell staining with HA antibody (anti-HA). HA-$\alpha_1$1.3-positive puncta (left, red) are present on the neuronal surface throughout the dendrites. A dendrite segment shown at higher magnification (right) reveals HA-$\alpha_1$1.3 puncta on the plasma membrane of dendritic spines (arrowheads). ***B***, Neuron (20 DIV) transfected with GFP-densin, double labeled with antibodies against GFP (anti-GFP, green) and the postsynaptic density protein 95 (anti-PSD95, red). Immunofluorescence for GFP was required due to the weak intrinsic fluorescence of GFP-densin. GFP-densin and PSD95 display similar clustered distributions throughout the dendrites. At higher magnification (right), there is strong colocalization of GFP-densin (green) with PSD95 (red; arrowheads). Scale bars: left, 20 μm; right, 5 μm. ***C–E***, Coimmunoprecipitation of densin, CaMKII, and $\alpha_1$1.3. Mouse hippocampal lysates were incubated with control goat IgG or affinity purified goat antibodies against $\alpha_1$1.3 (***C***), densin (***D***), or CaMKII (***E***). Coimmunoprecipitated proteins are indicated by arrows in Western blots for $\alpha_1$1.3 (top), densin (middle), or CaMKII (bottom). Input lanes (In) represent 5% of lysates used in the assay.

cantly less, with amplitudes at the end of the 300 ms train that were ~45% greater than in cells with $Ca_v1.3$ alone (Fig. 4*A*,*C*). The enhancement of I_{Ca} was independent of changes in voltage-dependent activation or peak current amplitude, which were not different in cells transfected with $Ca_v1.3$ alone ($k = -12.0 \pm 1.0$; $V_{1/2} = -7.1 \pm 0.3$; I_{Ca} amplitude at -10 mV = 1298.9 ± 304.6 pA; $n = 9$) and $Ca_v1.3$ plus densin plus CaMKII ($k = -12.5 \pm 2.2$, $p = 0.68$; $V_{1/2} = -7.2 \pm 0.5$, $p = 0.34$; I_{Ca} amplitude at -10 mV = 649.4 ± 165.2 pA, $p = 0.21$; $n = 10$; by *t* test).

To determine whether the effect of densin plus CaMKII was Ca^{2+} dependent, we analyzed I_{Ba}. Because Ba^{2+} does not support Ca^{2+}-dependent inactivation, the amplitude of I_{Ba} remains relatively constant throughout the train (Fig. 4*B*). In contrast to effects on I_{Ca}, densin plus CaMKII modestly increased inactivation of I_{Ba} (~11.8%) (Fig. 4*B*,*C*). The effects of densin plus CaMKII were not seen when densin or CaMKII was singly cotransfected with $Ca_v1.3$ (Fig. 4*C*). These results reveal that $Ca_v1.3$ currents undergo CDF during repetitive stimuli, which requires both densin and CaMKII.

Densin binding to the $\alpha_1$1.3 CT and CaMKII is required for CDF of $Ca_v1.3$

Since densin binds both $\alpha_1$1.3 CT (Fig. 2*C*,*D*) and CaMKII (Strack et al., 2000; Walikonis et al., 2001), we hypothesized that CDF requires densin to scaffold CaMKII to the $\alpha_1$1.3 CT. If so, then preventing these interactions should block CDF. We tested this prediction first with $\alpha_1$1.3 containing the L-A mutation, which prevents densin binding (Fig. 2*D*). As expected, there was no significant effect of densin plus CaMKII on I_{Ca} inactivation for channels containing the L-A mutation ($p = 0.15$) (Fig. 5*A*). We next examined the effect of deleting the PDZ domain from densin (ΔPDZ), which should also prevent binding to $\alpha_1$1.3 CT. Unlike full-length densin, the ΔPDZ truncation did not affect I_{Ca} amplitude at the end of the train ($p = 0.82$ compared with $Ca_v1.3$ alone) (Fig. 5*B*). Together, these data confirm the requirement for densin binding to $\alpha_1$1.3 CT for CDF.

CaMKII directly interacts with the C-terminal domain of densin *in vitro* (Fig. 2*A*) (Strack et al., 2000; Walikonis et al., 2001) and this interaction is sufficient for coimmunoprecipitation of CaMKII with densin from transfected HEK293 cells (Jiao et al., 2008). In ongoing studies to define domains in full-length densin that are necessary for interaction with CaMKII, we found that a large internal deletion (Δ483-1377) in a naturally occurring densin splice variant substantially reduces the coimmunoprecipitation of CaMKII when compared with the full-length densin (Fig. 5*C*). Apparently, the deleted region (Δ483-1377) is required for CaMKII binding. Since the Δ483-1377 densin variant retains the

PDZ domain and can bind to the $\alpha_1$1.3 CT in pull-down assays (data not shown), we used it to determine whether weakened interactions of densin with CaMKII affect CDF. In contrast to full-length densin, the Δ483-1377 variant did not support CDF of $Ca_v1.3$ I_{Ca} during repetitive stimuli ($p = 0.16$ compared with $Ca_v1.3$ alone) (Fig. 5*D*). Thus, our results support a mechanism in which densin recruits CaMKII to the $\alpha_1$1.3 CT, which promotes CDF of $Ca_v1.3$.

$Ca_v1.3$ CDF requires CaMKII activation

To probe further the relevance of CaMKII activity for $Ca_v1.3$ CDF, we used the CaMKII inhibitor, KN93, which blocks CaMKII activation by competing for the binding of Ca^{2+}/calmodulin. Since long incubations (1–2 h) with extracellular KN93 (10 μM) nonspecifically inhibit $Ca_v1.3$ channels independent of CaMKII (Gao et al., 2006a), we included KN93 in the intracellular solution, which did not affect the amplitude or other properties of $Ca_v1.3$ currents (supplemental Table 1, available at www.jneurosci.org as supplemental material). However, KN93 prevented the effect of densin and CaMKII on CDF, whereas the inactive analog, KN92, had no effect (Fig. 6*A*). We also tested the effect of inhibiting CaMKII by directly blocking the active site with CaM-KIINtide, a peptide derived from the naturally occurring CaMKII inhibitor protein, CaM-KIIN (Chang et al., 1998). CaM-KIINtide (10 μM), introduced via the patch electrode in cells cotransfected with $Ca_v1.3$ plus densin plus CaMKII, also inhibited $Ca_v1.3$ CDF: this group was not significantly different from cells transfected with $Ca_v1.3$ alone (Fig. 6*B*). We also tested the effect of mutating threonine286 to alanine (T286A) in CaMKII, which prevents autonomous kinase activity after dissociation of Ca^{2+}-calmodulin from CaMKII (Soderling, 1996). The T286A mutant, when coexpressed with densin and $Ca_v1.3$ did not support CDF (Fig. 6*C*). These results confirm that CaMKII activation and autonomous activity is necessary for $Ca_v1.3$ CDF.

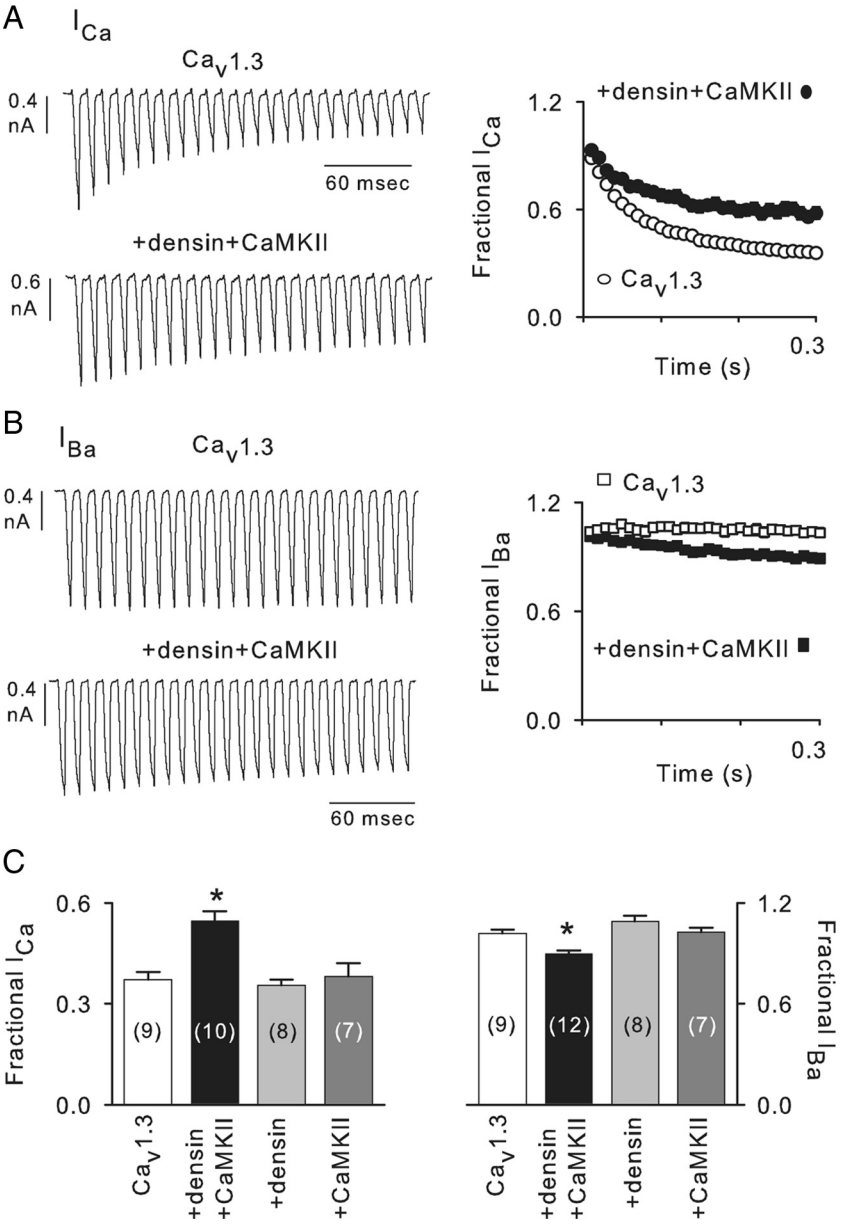

Figure 4. ***A***, ***B***, Densin and CaMKII cause CDF of $Ca_v1.3$. I_{Ca} (***A***) and I_{Ba} (***B***) were evoked by 5 ms pulses from −90 to −10 mV at 100 Hz in cells transfected with $Ca_v1.3$ alone ($\alpha_1$1.3, β_{1b}, $\alpha_2\delta$; $n = 9$ both for I_{Ca} and I_{Ba}) or cotransfected with densin plus CaMKII ($n = 10$ for I_{Ca}; $n = 12$ for I_{Ba}). Test current amplitudes were normalized to the first in the train (fractional current) and plotted against time (right). ***C***, Quantitation of data in ***A*** and ***B***. Fractional I_{Ca} and I_{Ba} for the last 11 pulses of the train were averaged for cells transfected with $Ca_v1.3$ alone, plus densin plus CaMKII, plus densin, or plus CaMKII. Parentheses indicate numbers of cells. *$p < 0.05$ compared with each group, by one-way ANOVA and Bonferroni's *post hoc* test.

The densin-dependent positioning of CaMKII within the channel complex may allow for local activation of CaMKII by Ca^{2+} that emerges from the pore of individual $Ca_v1.3$ channels. If so, there should be little reliance of CDF on macroscopic current amplitude, since only the single-channel current would be relevant. Alternatively, CDF may depend on a Ca^{2+} microdomain due to Ca^{2+} influx through, and accumulation near, neighboring channels. In this case, CDF should be greater for large- than for small-amplitude currents. To distinguish between these mechanisms, we separately analyzed cells with small (<250 pA)- and large (>250 pA)-amplitude currents. We found that CDF due to densin and CaMKII was significant only for the large-amplitude I_{Ca} (Fig. 7*A*,*B*), which supported the importance of a Ca^{2+} microdomain for CDF. However, Ca_v β subunits potentiate peak current amplitude (Perez-Reyes et al., 1992) and influence CaMKII regulation of $Ca_v1.2$ (Grueter et al., 2006, 2008; Abiria and Colbran, 2010). Thus, insensitivity of small currents to densin and CaMKII could have been related to low levels of Ca_v β expression. If so, small currents should show activation voltages that are positively shifted relative to large currents, since all Ca_v β subunits cause a negative shift in activation voltage of Ca_v1 channels (Perez-Reyes et al., 1992). There was no difference in voltage-dependent activation of small- and large-amplitude currents in cells with $Ca_v1.3$ alone or cotransfected with densin and CaMKII (supplemental Table 2, available at www.

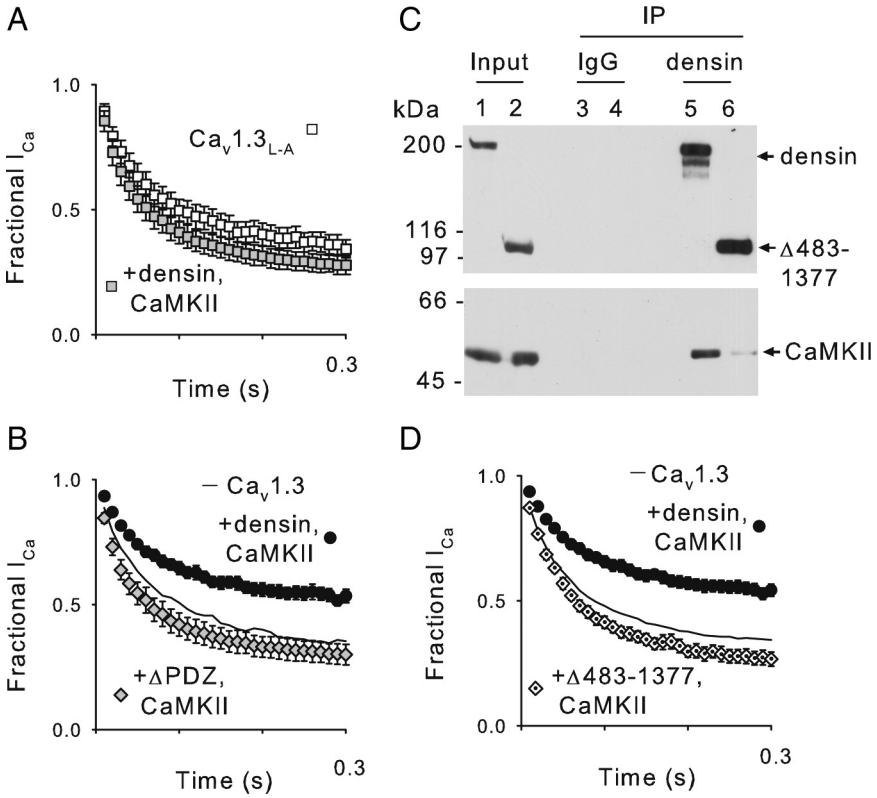

Figure 5. Densin binding to $\alpha_1$1.3 and CaMKII is required for $Ca_v1.3$ modulation. ***A***, ***B***, Fractional current for I_{Ca} was measured as in Fig. 4 for $Ca_v1.3$ ($\alpha_1 1.3_{L\text{-}A}$, β_{1b}, $\alpha_2\delta$) with mutated PDZ-binding site ($Ca_v1.3_{L\text{-}A}$, $n = 8$) alone or cotransfected with densin plus CaMKII ($n = 7$) (***A***); or wild-type $Ca_v1.3$ alone ($\alpha_1 1.3$, β_{1b}, $\alpha_2\delta$; $n = 9$) or cotransfected with densin plus CaMKII ($n = 11$), or with densin lacking PDZ domain (ΔPDZ) plus CaMKII ($n = 8$) (***B***). ***C***, Coimmunoprecipitation of CaMKII with densin but not densin with internal deletion (Δ483-1377). Transfected HEK293 cell lysates were incubated with control IgG (lanes 3 and 4) or antibodies against densin (lanes 5 and 6). Input lanes (1 and 2) represent ~5% of cell lysate used for coimmunoprecipitation. Western blotting was with antibodies against densin (top) or CaMKII (bottom). ***D***, Same as in ***A*** and ***B*** but for cells transfected with $Ca_v1.3$ alone ($n = 9$) or cotransfected with densin plus CaMKII ($n = 11$) or plus Δ483-1377 plus CaMKII ($n = 7$). Statistical differences described in text were determined by *t* test (***A***) or one-way ANOVA with Bonferroni's *post hoc* test (***B***, ***D***).

jneurosci.org as supplemental material), which showed that small currents arose from the same $Ca_v1.3$ subunit composition as large currents.

The Ca^{2+} dependence of CDF was further investigated by altering intracellular Ca^{2+} buffering strength. For this purpose, we substituted EGTA (5 mM) in the intracellular recording solution with BAPTA (10 mM). Due to its faster Ca^{2+} binding kinetics compared with EGTA (Tsien, 1980), BAPTA should more quickly nullify Ca^{2+} increases that support CDF. BAPTA even at 10 mM concentration, is permissive for Ca^{2+}-dependent inactivation of $Ca_v1.3$ (Dick et al., 2008), which depends on nanodomain Ca^{2+} signals emanating from individual channels. If CDF depends on a similar Ca^{2+} nanodomain, BAPTA should spare CDF. However, BAPTA effectively blunted the effects of densin and CaMKII on $Ca_v1.3$ CDF (Fig. 7*C*). Together, these results show that $Ca_v1.3$ CDF requires a Ca^{2+} microdomain that is supported by multiple open channels.

$Ca_v1.3$ CDF requires high-frequency stimulation

The activity of CaMKII depends on the frequency of Ca^{2+} transients in excitable cells (Meyer et al., 1992; Hanson et al., 1994; De Koninck and Schulman, 1998). High-frequency Ca^{2+} spikes limit Ca^{2+}/calmodulin dissociation, thus enhancing CaMKII autophosphorylation, which supports autonomous enzymatic activity (De Koninck and Schulman, 1998; Hudmon and Schulman, 2002). If frequency-dependent modulation of CaMKII contributes to $Ca_v1.3$ CDF, the effects of densin and CaMKII should be reduced during sustained or low-frequency depolarizations. Alternatively, if CDF depends only on a single Ca^{2+} burst due to rapid opening of $Ca_v1.3$ channels, CaMKII and densin should still facilitate $Ca_v1.3$ I_{Ca} evoked by sustained or low-frequency depolarizations. To distinguish between these possibilities, we first analyzed I_{Ca} during a 300 ms step depolarization. The ratio of the residual amplitude of I_{Ca} at the end of the pulse normalized to the peak current amplitude (I_{res}/I_{peak}) (Fig. 8*A*) provided a metric analogous to that used for assessing CDF at the end of the 100 Hz train (Fig. 4*A*). If repetitive depolarizations are necessary for CDF, densin and CaMKII should not influence I_{res}/I_{peak}. In cells transfected with $Ca_v1.3$ alone, I_{res}/I_{peak} for I_{Ca} shows U-shaped dependence on test voltage due to Ca^{2+}-dependent inactivation (Brehm and Eckert, 1978). Interestingly, densin plus CaMKII actually increased inactivation at a more positive voltages (+30 mV, $I_{res}/I_{peak} = 0.0.26 \pm 0.03$ for $Ca_v1.3$ alone, $n = 7$ vs 0.15 ± 0.03 for $Ca_v1.3$ plus densin plus CaMKII, $n = 13$; $p < 0.05$) (Fig. 8*A*). This appears to result from enhanced voltage-dependent inactivation by densin plus CaMKII, which was evident as increased inactivation of I_{Ba} in triply transfected cells during repetitive and sustained depolarizations (Fig. 4*B*,*C*; supplemental Fig. 2, available at www.jneurosci.org as supplemental material). However, with all other test voltages, including the same voltage used in the 100 Hz protocol (−10 mV) (Figs. 4, 5), I_{res}/I_{peak} was not significantly different in cells transfected with $Ca_v1.3$ alone and those cotransfected with densin plus CaMKII (Fig. 8*A*). This result demonstrates that a sustained depolarization is insufficient to produce $Ca_v1.3$ CDF.

High-frequency activation of $Ca_v1.3$ channels may trigger the rapid accumulation of Ca^{2+} that facilitates Ca^{2+}/calmodulin binding to CaMKII, autophosphorylation of the kinase at Thr286, and changes in channel gating that underlie CDF. Due to Ca^{2+} diffusion from microdomains supporting CDF, low-frequency activation of $Ca_v1.3$ channels may be less effective in promoting autonomous CaMKII activity. To test this, we characterized CDF during 50 Hz trains of depolarizations. As expected, there was no significant effect of densin and CaMKII on CDF with this voltage protocol, even for long (1 s) trains ($p = 0.77$ compared with 100 Hz stimulation) (Fig. 8*B*). To further define the Ca^{2+} signal that underlies CDF, we performed simultaneous electrophysiological and optical recordings with the ratiometric Ca^{2+} indicator fura-2, which was introduced into cells via the patch electrode. These experiments showed that within the 300 ms train, stimulation at 100 Hz caused a significantly greater (~32%) and faster (~39%) increase in Ca^{2+} compared with 50 Hz (Fig. 8*C*,*D*). Together, these data highlight the impor-

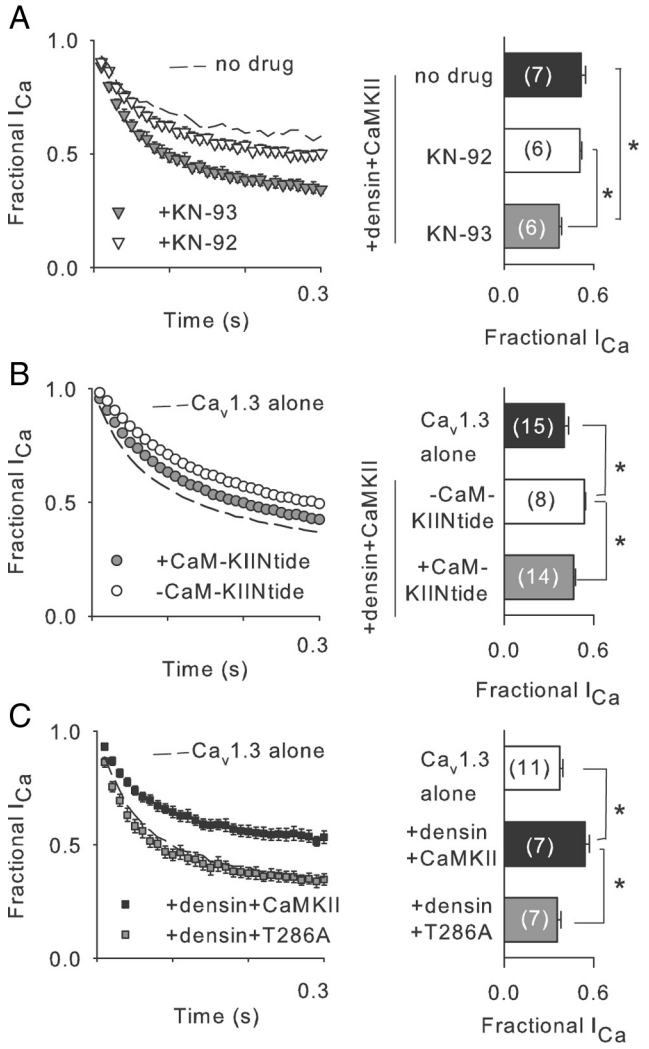

Figure 6. CaMKII activation and autophosphorylation are required for $Ca_v1.3$ CDF. ***A–C***, Left, Fractional I_{Ca} was measured as in Fig. 4 for I_{Ca} for cells transfected with $Ca_v1.3$ alone ($\alpha_1$1.3, β_{1b}, $\alpha_2\delta$) or cotransfected with densin and CaMKII. Right, Average fractional I_{Ca} for the last 11 pulses. ***A***, ***B***, KN-93 (10 μM) but not KN-92 (10 μM) in the intracellular recording solution inhibited CDF (***A***) as did CaM-KIINtide (***B***, 10 μM). For ***B***, $^*p < 0.05$ by Kruskal–Wallis ANOVA on ranks and Dunn's *post hoc* test. Results for plus CaM-KIINtide were not significantly different from $Ca_v1.3$ alone. ***C***, CaMKII autophosphorylation mutant (T286A) inhibited CDF. Parentheses indicate number of cells. For ***A*** and ***C***, $^*p < 0.01$ by one-way ANOVA and Bonferroni's *post hoc* analysis.

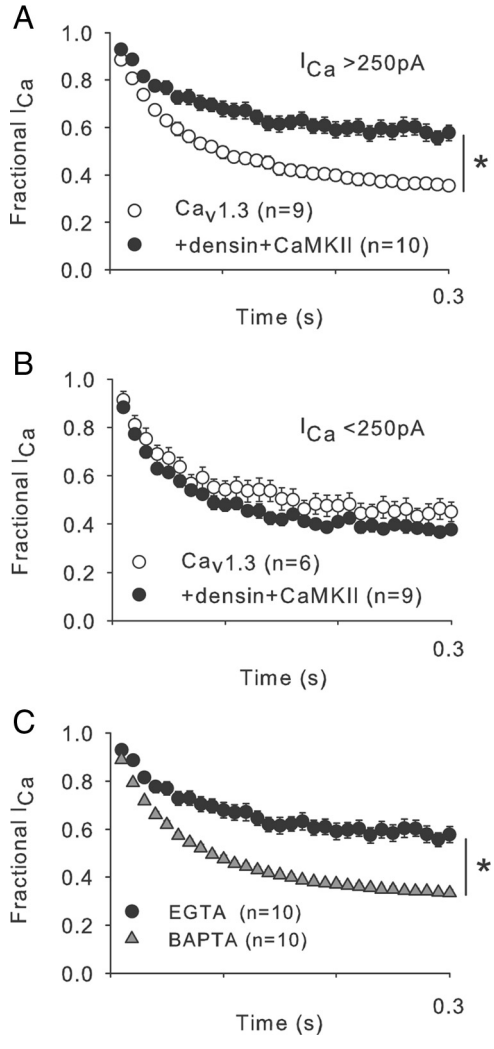

Figure 7. $Ca_v1.3$ CDF is blunted for low-amplitude I_{Ca} and intracellular BAPTA. ***A–C***, Fractional I_{Ca} was measured as in Fig. 4 for I_{Ca} for cells transfected with $Ca_v1.3$ alone ($\alpha_1$1.3, β_{1b}, $\alpha_2\delta$) or cotransfected with densin and CaMKII for I_{Ca} with amplitude >250 pA (***A***) or <250 pA (***B***) or with EGTA or BAPTA in the intracellular solution (***C***). Average fractional I_{Ca} for last 11 pulses was compared by *t* test ($^*p < 0.001$; in ***B***, $^*p = 0.14$).

tance of high-frequency stimulation for fast and robust increases in Ca^{2+} that support $Ca_v1.3$ CDF.

Discussion

Our results reveal a novel feedback regulation of $Ca_v1.3$ channels that involves multivalent interactions between $Ca_v1.3$ α_1 subunits, densin, and CaMKII. Densin binding to the distal C-terminal domain of $\alpha_1$1.3 permits CaMKII-dependent facilitation of $Ca_v1.3$ Ca^{2+} currents during high-frequency, depolarizing stimuli. This regulation depends on precise patterns of $Ca_v1.3$ Ca^{2+} influx, CaMKII binding to densin, and CaMKII autophosphorylation. Association of $Ca_v1.3$, densin, and CaMKII at some synapses may coordinate activity-dependent potentiation of L-type Ca^{2+} currents underlying alterations in synaptic efficacy and other neuronal functions.

Ca^{2+}-dependent facilitation of $Ca_v1.3$ by densin and CaMKII

The regulation of voltage-gated (Ca_v) Ca^{2+} channels by permeating Ca^{2+} ions permits fast and efficient control of Ca^{2+} signals in excitable cells. CDI curtails Ca^{2+} influx and is mediated by CaM binding to the proximal C-terminal domain of the Ca_v α_1 subunit (Halling et al., 2006). CDF boosts Ca^{2+} entry through Ca_v channels, but via multiple mechanisms. For $Ca_v1.2$, CDF involves CaMKII binding to and phosphorylation of α_1 and/or β subunits (Hudmon et al., 2005; Grueter et al., 2006). However, in recombinant systems, CDF of whole-cell $Ca_v1.2$ currents is not evident unless CDI is first inhibited by mutations of the CaM binding (IQ) domain (Zühlke et al., 1999, 2000). In contrast, $Ca_v1.2$ channels in cardiac myocytes undergo overt CDF (Noble and Shimoni, 1981; Marban and Tsien, 1982; Lee, 1987), suggesting that additional factors are permissive for CDF of native $Ca_v1.2$ channels. We also did not detect CDF for $Ca_v1.3$ transfected alone or cotransfected only with CaMKII in HEK293Tcells (Fig. 4). Due to CDI, $Ca_v1.3$ I_{Ca} showed only inactivation during 100 Hz depolarizations (Fig. 4*A*). However, we interpret the enhanced I_{Ca} amplitudes in cells cotransfected with densin and CaMKII (Fig. 4*A*,*C*) as CDF, which overlaps temporally with

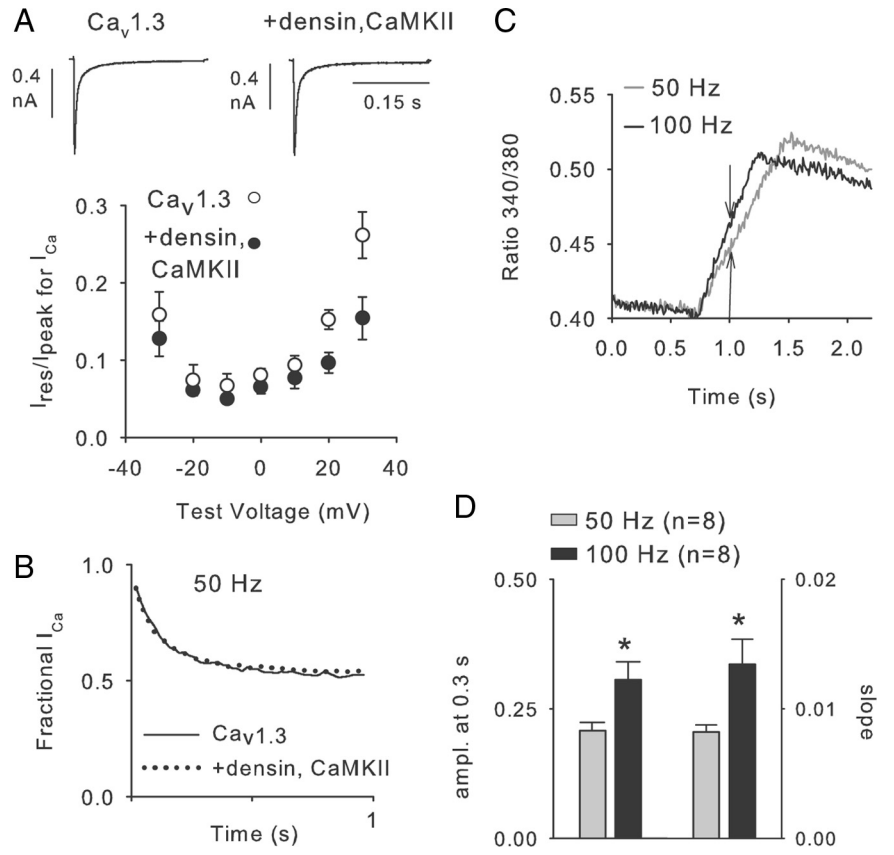

Figure 8. Densin and CaMKII do not cause CDF during sustained or low-frequency depolarizations. ***A***, I_{Ca} was evoked by 300 ms step pulses from −90 mV to various voltages. I_{res}/I_{peak} was plotted against test voltage (bottom) for $Ca_v1.3$ ($\alpha_1$1.3, β_{1b}, $\alpha_2\delta$) alone ($n = 7$) or $Ca_v1.3$ plus densin plus CaMKII ($n = 13$). Except for at +30 mV, there was no difference in I_{res}/I_{peak} for $Ca_v1.3$ alone or cotransfected with densin and CaMKII by two-way ANOVA and Bonferroni's *post hoc* test. ***B***, Fractional I_{Ca} obtained from 50 Hz depolarizations (5 ms pulses from −90 to −10 mV) for $Ca_v1.3$ alone ($n = 14$) or cotransfected with densin plus CaMKII ($n = 18$). By *t* test, there was no difference in fractional I_{Ca} for last 11 pulses for $Ca_v1.3$ alone (0.54 ± 0.03) or plus densin plus CaMKII (0.55 ± 0.02; $p = 0.62$). ***C***, ***D***, Intracellular Ca^{2+} signals in HEK293T cells cotransfected with $Ca_v1.3$, densin, and CaMKII measured by fura-2. Transfected cells were subject to simultaneous whole-cell patch-clamp recording of I_{Ca} and imaging of fura-2 fluorescence. ***C***, Representative traces show Ca^{2+} signal measured as the ratio of fura-2 fluorescence from excitation at 340 and 380 nm following 50 or 100 Hz stimulation. ***D***, The signal amplitude at 0.3 s (indicated by arrows in ***C***) was normalized to whole-cell current amplitude to control for differences in current density between cells and compared by *t* test (*$p = 0.02$ by *t* test). The slope of the traces was compared by Mann–Whitney rank sum test (*$p = 0.007$).

CDI during the 100 Hz train. Facilitation was Ca^{2+} dependent since it was seen for I_{Ca} and not I_{Ba} (Fig. 4*B*), increased with I_{Ca} amplitude (Fig. 7*A*,*B*), and was inhibited by BAPTA in the intracellular recording solution (Fig. 7*C*).

Our results indicate that densin scaffolds CaMKII to the $\alpha_1$1.3 CT, which enables local activation of CaMKII by Ca^{2+}/calmodulin. The ability of CaMKII to respond to the frequency of Ca^{2+} oscillations with different levels of activity is well established (De Koninck and Schulman, 1998) and involves Ca^{2+}/calmodulin-stimulated autophosphorylation at Thr286 of individual subunits, 12 of which form the CaMKII holoenzyme (Hudmon and Schulman, 2002). The importance of high-frequency depolarizations and CaMKII Thr286 autophosphorylation in our experiments (Figs. 6*C*, 8) implies that CDF requires CaMKII catalytic activity. Potential substrates for CaMKII phosphorylation include densin (Strack et al., 2000; Walikonis et al., 2001). In addition, CaMKII may phosphorylate the $Ca_v\beta$ subunit (Grueter et al., 2008), which increases the open probability of cardiac $Ca_v1.2$ channels (Grueter et al., 2006). Finally, CaMKII could phosphorylate $\alpha_1$1.3. In SHSY5Y cells and cortical neurons, CaMKII-dependent enhancement of $Ca_V1.3$ following stimulation with insulin like growth factor 1 is prevented by mutation of Ser1486 in $\alpha_1$1.3 to Ala (Gao et al., 2006b), although it has not been shown that CaMKII directly phosphorylates Ser1486. Moreover, insulin like growth factor 1 enhanced Ba^{2+} currents carried by $Ca_V1.3$ channels by shifting voltage-dependent activation of the channel to more negative voltages, independent of repetitive stimulation. Thus, the CaMKII- and densin-dependent CDF in our experiments appears quite distinct from previously described modes of $Ca_v1.3$ regulation. Further studies will be necessary to dissect the molecular targets of CaMKII and their involvement in CDF and other forms of $Ca_v1.3$ modulation.

Densin as a scaffold for CaMKII in the $Ca_v1.3$ channel complex

Densin interacts with a number of postsynaptic proteins, including Shank (Quitsch et al., 2005), δ-catenin (Martinez et al., 2003), and α-actinin (Walikonis et al., 2001; Robison et al., 2005), but how densin influences these proteins is generally not known. Our results indicate that densin may scaffold CaMKII to postsynaptic $Ca_v1.3$ channels, much like A-kinase anchoring proteins tether PKA (Hulme et al., 2003) and calcineurin (Oliveria et al., 2007) to $Ca_v1.2$. This mechanism allows for fast and efficient modulation of Ca_v1 channels, which is consistent with the millisecond time course of $Ca_v1.3$ facilitation we found in our experiments (Fig. 4*A*). At the same time, CaMKII is also a transducer of Ca_v1 Ca^{2+} signals. For example, CaMKII responds to Ca_v1 channel opening by forming clusters at the neuronal plasma membrane and selectively couples Ca_v1 but not Ca_v2 channels to pCREB activation in response to moderate depolarizations (Wheeler et al., 2008). Ca_v2 channels are not likely to bind densin since they lack a type I PDZ-binding sequence. Association of densin and CaMKII with $Ca_v1.3$ in the brain (Fig. 3*C–E*) may therefore contribute to the Ca_v1-specific nature of pCREB signaling (Zhang et al., 2006).

Although CDF due to densin and CaMKII was only seen for large-amplitude currents recorded in high concentrations of extracellular Ca^{2+} (10 mM) during intense depolarizing stimuli, we predict that $Ca_v1.3$ CDF due to densin and CaMKII will be physiologically relevant in neurons. $Ca_v1.3$ and densin are concentrated in dendritic spines (Fig. 3*A*), which have a relatively small volume, particularly compared with HEK293T cells. Previous work shows that $Ca_v1.2$ channels are clustered in spines, in which it was estimated that there are ~8 channels per cluster (Obermair et al., 2004). Similar clustering of $Ca_v1.3$ channels within spines, which is suggested by the immunofluorescence of HA-$\alpha_1$1.3 (Fig. 3*A*) (Gao et al., 2006b), should efficiently produce the Ca^{2+} microdomain required for CDF even under physiological (<2 mM) extracellular Ca^{2+} concentrations. During stimuli that promote long-term potentiation, CaMKII activation in den-

dritic spines is mediated by Ca_v1 channels and is blocked by 20 mM BAPTA but partially spared by the same concentration of EGTA (Lee et al., 2009). In this context, densin and CaMKII may endow $Ca_v1.3$ channels with a positive feedback regulation to boost local Ca^{2+} signals that initiate CaMKII activation and participation in long-term synaptic plasticity.

However, densin and CaMKII may also underlie pathological changes associated with hyperactivation of $Ca_v1.3$ channels. For example, in the striatum, the excitability of striatopallidal neurons is regulated by $Ca_v1.3$ channels, which are inhibited by D_2 dopamine receptors (Olson et al., 2005). Excessive Ca^{2+} influx via $Ca_v1.3$ channels following dopamine depletion results in a loss of dendritic spines in striatopallidal neurons, since these morphological changes are not seen in mice lacking $Ca_v1.3$ (Day et al., 2006). Intriguingly, CaMKII activity is also upregulated upon dopamine depletion (Picconi et al., 2004; Brown et al., 2005), which may further exacerbate Ca^{2+} overloads by promoting $Ca_v1.3$ CDF. Moreover, CaMKII inhibition alleviates defects in synaptic plasticity and motor deficits following striatal dopamine depletion (Picconi et al., 2004). Thus, elucidating the functional relationships between densin, CaMKII, and $Ca_v1.3$ at striatopallidal synapses may yield further insights into the potential therapeutic efficacy of $Ca_v1.3$ blockers for Parkinson's disease (Chan et al., 2007, 2009).

References

Abiria SA, Colbran RJ (2010) CaMKII associates with $Ca_v1.2$ L-type calcium channels via selected beta subunits to enhance regulatory phosphorylation. J Neurochem 112:150–161.

Altier C, Dubel SJ, Barrère C, Jarvis SE, Stotz SC, Spaetgens RL, Scott JD, Cornet V, De Waard M, Zamponi GW, Nargeot J, Bourinet E (2002) Trafficking of L-type calcium channels mediated by the postsynaptic scaffolding protein AKAP79. J Biol Chem 277:33598–33603.

Apperson ML, Moon IS, Kennedy MB (1996) Characterization of densin-180, a new brain-specific synaptic protein of the *O*-sialoglycoprotein family. J Neurosci 16:6839–6852.

Bilder D, Birnbaum D, Borg JP, Bryant P, Huigbretse J, Jansen E, Kennedy MB, Labouesse M, Legouis R, Mechler B, Perrimon N, Petit M, Sinha P (2000) Collective nomenclature for LAP proteins. Nat Cell Biol 2:E114.

Brehm P, Eckert R (1978) Calcium entry leads to inactivation of calcium channel in *Paramecium*. Science 202:1203–1206.

Brickey DA, Colbran RJ, Fong YL, Soderling TR (1990) Expression and characterization of the alpha-subunit of Ca^{2+}/calmodulin-dependent protein kinase II using the baculovirus expression system. Biochem Biophys Res Commun 173:578–584.

Brown AM, Deutch AY, Colbran RJ (2005) Dopamine depletion alters phosphorylation of striatal proteins in a model of Parkinsonism. Eur J Neurosci 22:247–256.

Calin-Jageman I, Lee A (2008) Ca_v1 L-type Ca^{2+} channel signaling complexes in neurons. J Neurochem 105:573–583.

Calin-Jageman I, Yu K, Hall RA, Mei L, Lee A (2007) Erbin enhances voltage-dependent facilitation of $Ca_v1.3$ Ca^{2+} channels through relief of an autoinhibitory domain in the $Ca_v1.3$ α_1 subunit. J Neurosci 27:1374–1385.

Chan CS, Guzman JN, Ilijic E, Mercer JN, Rick C, Tkatch T, Meredith GE, Surmeier DJ (2007) 'Rejuvenation' protects neurons in mouse models of Parkinson's disease. Nature 447:1081–1086.

Chan CS, Gertler TS, Surmeier DJ (2009) Calcium homeostasis, selective vulnerability and Parkinson's disease. Trends Neurosci 32:249–256.

Chang BH, Mukherji S, Soderling TR (1998) Characterization of a calmodulin kinase II inhibitor protein in brain. Proc Natl Acad Sci U S A 95:10890–10895.

Colbran RJ, Brown AM (2004) Calcium/calmodulin-dependent protein kinase II and synaptic plasticity. Curr Opin Neurobiol 14:318–327.

Day M, Wang Z, Ding J, An X, Ingham CA, Shering AF, Wokosin D, Ilijic E, Sun Z, Sampson AR, Mugnaini E, Deutch AY, Sesack SR, Arbuthnott GW, Surmeier DJ (2006) Selective elimination of glutamatergic synapses on striatopallidal neurons in Parkinson disease models. Nat Neurosci 9:251–259.

De Koninck P, Schulman H (1998) Sensitivity of CaM kinase II to the frequency of Ca^{2+} oscillations. Science 279:227–230.

Dick IE, Tadross MR, Liang H, Tay LH, Yang W, Yue DT (2008) A modular switch for spatial Ca^{2+} selectivity in the calmodulin regulation of Ca_V channels. Nature 451:830–834.

Dzhura I, Wu Y, Colbran RJ, Balser JR, Anderson ME (2000) Calmodulin kinase determines calcium-dependent facilitation of L-type calcium channels. Nat Cell Biol 2:173–177.

Fam SR, Paquet M, Castleberry AM, Oller H, Lee CJ, Traynelis SF, Smith Y, Yun CC, Hall RA (2005) P2Y1 receptor signaling is controlled by interaction with the PDZ scaffold NHERF-2. Proc Natl Acad Sci U S A 102:8042–8047.

Gao L, Blair LA, Marshall J (2006a) CaMKII-independent effects of KN93 and its inactive analog KN92: reversible inhibition of L-type calcium channels. Biochem Biophys Res Commun 345:1606–1610.

Gao L, Blair LA, Salinas GD, Needleman LA, Marshall J (2006b) Insulin-like growth factor-1 modulation of $Ca_V1.3$ calcium channels depends on Ca^{2+} release from IP_3-sensitive stores and calcium/calmodulin kinase II phosphorylation of the α_1 subunit EF hand. J Neurosci 26:6259–6268.

Griffith LC (2004) Regulation of calcium/calmodulin-dependent protein kinase II activation by intramolecular and intermolecular interactions. J Neurosci 24:8394–8398.

Grueter CE, Abiria SA, Dzhura I, Wu Y, Ham AJ, Mohler PJ, Anderson ME, Colbran RJ (2006) L-type Ca^{2+} channel facilitation mediated by phosphorylation of the β subunit by CaMKII. Mol Cell 23:641–650.

Grueter CE, Abiria SA, Wu Y, Anderson ME, Colbran RJ (2008) Differential regulated interactions of calcium/calmodulin-dependent protein kinase II with isoforms of voltage-gated calcium channel beta subunits. Biochemistry 47:1760–1767.

Halling DB, Aracena-Parks P, Hamilton SL (2006) Regulation of voltage-gated Ca^{2+} channels by calmodulin. Sci STKE 2006:er1.

Hanson PI, Meyer T, Stryer L, Schulman H (1994) Dual role of calmodulin in autophosphorylation of multifunctional CaM kinase may underlie decoding of calcium signals. Neuron 12:943–956.

Helton TD, Xu W, Lipscombe D (2005) Neuronal L-type calcium channels open quickly and are inhibited slowly. J Neurosci 25:10247–10251.

Hudmon A, Schulman H (2002) Neuronal Ca^{2+}/calmodulin-dependent protein kinase II: the role of structure and autoregulation in cellular function. Annu Rev Biochem 71:473–510.

Hudmon A, Schulman H, Kim J, Maltez JM, Tsien RW, Pitt GS (2005) CaMKII tethers to L-type Ca^{2+} channels, establishing a local and dedicated integrator of Ca^{2+} signals for facilitation. J Cell Biol 171:537–547.

Hulme JT, Lin TW, Westenbroek RE, Scheuer T, Catterall WA (2003) Beta-adrenergic regulation requires direct anchoring of PKA to cardiac $Ca_v1.2$ channels via a leucine zipper interaction with A kinase-anchoring protein 15. Proc Natl Acad Sci U S A 100:13093–13098.

Hulme JT, Scheuer T, Catterall WA (2004) Regulation of cardiac ion channels by signaling complexes: role of modified leucine zipper motifs. J Mol Cell Cardiol 37:625–631.

Izawa I, Nishizawa M, Ohtakara K, Inagaki M (2002) Densin-180 interacts with delta-catenin/neural plakophilin-related armadillo repeat protein at synapses. J Biol Chem 277:5345–5350.

Jiao Y, Robison AJ, Bass MA, Colbran RJ (2008) Developmentally regulated alternative splicing of densin modulates protein-protein interaction and subcellular localization. J Neurochem 105:1746–1760.

Koschak A, Reimer D, Huber I, Grabner M, Glossmann H, Engel J, Striessnig J (2001) α_{1D} ($Ca_v1.3$) subunits can form L-type Ca^{2+} channels activating at negative voltages. J Biol Chem 276:22100–22106.

Lee KS (1987) Potentiation of the calcium-channel currents of internally perfused mammalian heart cells by repetitive depolarization. Proc Natl Acad Sci U S A 84:3941–3945.

Lee SJ, Escobedo-Lozoya Y, Szatmari EM, Yasuda R (2009) Activation of CaMKII in single dendritic spines during long-term potentiation. Nature 458:299–304.

Lee TS, Karl R, Moosmang S, Lenhardt P, Klugbauer N, Hofmann F, Kleppisch T, Welling A (2006) Calmodulin kinase II is involved in voltage-dependent facilitation of the L-type $Ca_v1.2$ calcium channel: identification of the phosphorylation sites. J Biol Chem 281:25560–25567.

Lisman J, Schulman H, Cline H (2002) The molecular basis of CaMKII function in synaptic and behavioural memory. Nat Rev Neurosci 3:175–190.

Marban E, Tsien RW (1982) Enhancement of calcium current during digi-

talis inotropy in mammalian heart: positive feed-back regulation by intracellular calcium? J Physiol 329:589–614.
Martinez MC, Ochiishi T, Majewski M, Kosik KS (2003) Dual regulation of neuronal morphogenesis by a delta-catenin-cortactin complex and Rho. J Cell Biol 162:99–111.
McKinney BC, Murphy GG (2006) The L-type voltage-gated calcium channel $Ca_v1.3$ mediates consolidation, but not extinction, of contextually conditioned fear in mice. Learn Mem 13:584–589.
McNeill RB, Colbran RJ (1995) Interaction of autophosphorylated Ca^{2+}/calmodulin-dependent protein kinase II with neuronal cytoskeletal proteins. Characterization of binding to a 190-kDa postsynaptic density protein. J Biol Chem 270:10043–10049.
Meyer T, Hanson PI, Stryer L, Schulman H (1992) Calmodulin trapping by calcium-calmodulin-dependent protein kinase. Science 256:1199–1202.
Noble S, Shimoni Y (1981) The calcium and frequency dependence of the slow inward current 'staircase' in frog atrium. J Physiol 310:57–75.
Obermair GJ, Szabo Z, Bourinet E, Flucher BE (2004) Differential targeting of the L-type Ca^{2+} channel α_{1C} ($Ca_v1.2$) to synaptic and extrasynaptic compartments in hippocampal neurons. Eur J Neurosci 19:2109–2122.
Obermair GJ, Schlick B, Di Biase V, Subramanyam P, Gebhart M, Baumgartner S, Flucher BE (2010) Reciprocal interactions regulate targeting of calcium channel β subunits and membrane expression of α_1 subunits in cultured hippocampal neurons. J Biol Chem 285:5776–5791.
Ohtakara K, Nishizawa M, Izawa I, Hata Y, Matsushima S, Taki W, Inada H, Takai Y, Inagaki M (2002) Densin-180, a synaptic protein, links to PSD-95 through its direct interaction with MAGUIN-1. Genes Cells 7:1149–1160.
Oliveria SF, Dell'Acqua ML, Sather WA (2007) AKAP79/150 anchoring of calcineurin controls neuronal L-type Ca^{2+} channel activity and nuclear signaling. Neuron 55:261–275.
Olson PA, Tkatch T, Hernandez-Lopez S, Ulrich S, Ilijic E, Mugnaini E, Zhang H, Bezprozvanny I, Surmeier DJ (2005) G-protein-coupled receptor modulation of striatal $Ca_V1.3$ L-type Ca^{2+} channels is dependent on a Shank-binding domain. J Neurosci 25:1050–1062.
Perez-Reyes E, Castellano A, Kim HS, Bertrand P, Baggstrom E, Lacerda AE, Wei XY, Birnbaumer L (1992) Cloning and expression of a cardiac/brain beta subunit of the L-type calcium channel. J Biol Chem 267:1792–1797.
Picconi B, Gardoni F, Centonze D, Mauceri D, Cenci MA, Bernardi G, Calabresi P, Di Luca M (2004) Abnormal Ca^{2+}-calmodulin-dependent protein kinase II function mediates synaptic and motor deficits in experimental parkinsonism. J Neurosci 24:5283–5291.
Puopolo M, Raviola E, Bean BP (2007) Roles of subthreshold calcium current and sodium current in spontaneous firing of mouse midbrain dopamine neurons. J Neurosci 27:645–656.
Quitsch A, Berhörster K, Liew CW, Richter D, Kreienkamp HJ (2005) Postsynaptic shank antagonizes dendrite branching induced by the leucine-rich repeat protein Densin-180. J Neurosci 25:479–487.
Robison AJ, Bass MA, Jiao Y, MacMillan LB, Carmody LC, Bartlett RK, Colbran RJ (2005) Multivalent interactions of calcium/calmodulin-dependent protein kinase II with the postsynaptic density proteins NR2B, densin-180, and alpha-actinin-2. J Biol Chem 280:35329–35336.
Rose J, Jin SX, Craig AM (2009) Heterosynaptic molecular dynamics: locally induced propagating synaptic accumulation of CaM kinase II. Neuron 61:351–358.
Scholze A, Plant TD, Dolphin AC, Nürnberg B (2001) Functional expression and characterization of a voltage-gated $Ca_V1.3$ (α_{1D}) calcium channel subunit from an insulin-secreting cell line. Mol Endocrinol 15:1211–1221.
Sinnegger-Brauns MJ, Hetzenauer A, Huber IG, Renström E, Wietzorrek G, Berjukov S, Cavalli M, Walter D, Koschak A, Waldschütz R, Hering S, Bova S, Rorsman P, Pongs O, Singewald N, Striessnig JJ (2004) Isoform-specific regulation of mood behavior and pancreatic beta cell and cardiovascular function by L-type Ca^{2+} channels. J Clin Invest 113:1430–1439.
Soderling TR (1996) Structure and regulation of calcium/calmodulin-dependent protein kinases II and IV. Biochim Biophys Acta 1297:131–138.
Songyang Z, Fanning AS, Fu C, Xu J, Marfatia SM, Chishti AH, Crompton A, Chan AC, Anderson JM, Cantley LC (1997) Recognition of unique carboxyl-terminal motifs by distinct PDZ domains. Science 275:73–77.
Strack S, Robison AJ, Bass MA, Colbran RJ (2000) Association of calcium/calmodulin-dependent kinase II with developmentally regulated splice variants of the postsynaptic density protein densin-180. J Biol Chem 275:25061–25064.
Tsien RY (1980) New calcium indicators and buffers with high selectivity against magnesium and protons: design, synthesis, and properties of prototype structures. Biochemistry 19:2396–2404.
Walikonis RS, Oguni A, Khorosheva EM, Jeng CJ, Asuncion FJ, Kennedy MB (2001) Densin-180 forms a ternary complex with the α-subunit of Ca^{2+}/calmodulin-dependent protein kinase II and α-actinin. J Neurosci 21:423–433.
Wheeler DG, Barrett CF, Groth RD, Safa P, Tsien RW (2008) CaMKII locally encodes L-type channel activity to signal to nuclear CREB in excitation-transcription coupling. J Cell Biol 183:849–863.
Wu Y, Dzhura I, Colbran RJ, Anderson ME (2001) Calmodulin kinase and a calmodulin-binding 'IQ' domain facilitate L-type Ca^{2+} current in rabbit ventricular myocytes by a common mechanism. J Physiol 535:679–687.
Xu W, Lipscombe D (2001) Neuronal $Ca_v1.3$ α_1 L-type channels activate at relatively hyperpolarized membrane potentials and are incompletely inhibited by dihydropyridines. J Neurosci 21:5944–5951.
Yang PS, Alseikhan BA, Hiel H, Grant L, Mori MX, Yang W, Fuchs PA, Yue DT (2006) Switching of Ca^{2+}-dependent inactivation of $Ca_v1.3$ channels by calcium binding proteins of auditory hair cells. J Neurosci 26:10677–10689.
Yasuda R, Sabatini BL, Svoboda K (2003) Plasticity of calcium channels in dendritic spines. Nat Neurosci 6:948–955.
Zhang H, Fu Y, Altier C, Platzer J, Surmeier DJ, Bezprozvanny I (2006) $Ca_V1.2$ and $Ca_V1.3$ neuronal L-type calcium channels: differential targeting and signaling to pCREB. Eur J Neurosci 23:2297–2310.
Zühlke RD, Pitt GS, Deisseroth K, Tsien RW, Reuter H (1999) Calmodulin supports both inactivation and facilitation of L-type calcium channels. Nature 399:159–162.
Zühlke RD, Pitt GS, Tsien RW, Reuter H (2000) Ca^{2+}-sensitive inactivation and facilitation of L-type Ca^{2+} channels both depend on specific amino acid residues in a consensus calmodulin-binding motif in the α_{1C} subunit. J Biol Chem 275:21121–21129.